Published by Avanti Publishers

International Journal of Petroleum Technology

ISSN (online): 2409-787X

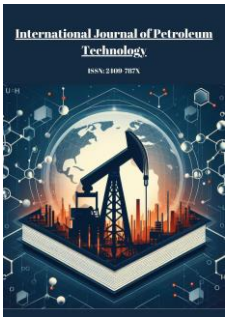

Quantitative Experimental Analysis of Controlling Factors on Waterflood Efficiency in Low-Permeability Reservoirs

Shijie Zhu[1,2], Zhonghua Liu[1,3,*], Yuedi Wang[1], Yiqiang Pan[1], Heng Zhang[4], Xiaoqing Wang[5] and Xijin Wang[6]

[1]Chongqing University of Science and Technology, College of Petroleum and Natural Gas Engineering, Chongqing 401331, China; [2]Chongqing Key Laboratory of Complex Oil and Gas Field Exploration and Development, Chongqing 401331, China; [3]Chongqing Key Laboratory of Efficient and Green Unconventional Oil and Gas Development, Chongqing 401331, China; [4]CNOOC Energy Development Co., Ltd. Engineering Technology Zhanjiang Branch, Zhanjiang, Guangdong 524000, China; [5]Sichuan Nengtou Oil and Gas Exploration and Development Co., Ltd, Sichuan, Chengdu 610000, China; [6]Sichuan Nengtou Tianfu Oil and Gas Exploration and Development Co., Ltd, Sichuan, Chengdu 610000, China

ARTICLE INFO

Article Type: Research Article

Academic Editor: Shenglai Guo

Keywords:
Enhanced oil recovery,
Reservoir heterogeneity,
Waterflooding efficiency,
Threshold pressure gradient,
Low-permeability reservoirs.

Timeline:
Received: March 07, 2026
Accepted: April 10, 2026
Published: April 25, 2026

Citation: Zhu S, Liu Z, Wang Y, Pan Y, Zhang H, Wang X, Wang X. Quantitative experimental analysis of controlling factors on waterflood efficiency in low-permeability reservoirs. Int J Pet Technol. 2026; 13(1): 17-28.

DOI: https: //doi.org/10.15377/2409-787X.2026.13.2

ABSTRACT

Revealing dominant controls on waterflood efficiency in low-permeability reservoirs is critical for optimizing development strategies and enhancing recovery. This study investigates a low-permeability reservoir through core analysis and displacement experiments, examining threshold pressure gradients and the impacts of permeability variation, pressure differential, and displacing velocity on flood performance. Key findings indicate: 1) A power-law correlation between threshold pressure gradient (G) and permeability (K) in reservoir cores: $G = 1.7707 \times K^{-0.339}$ (R^2 = 0.9246), demonstrating significant crude oil mobilization resistance. 2) At permeability gradients ≥4, low-permeability zones exhibit negligible crude oil displacement. Water injection preferentially channels through high-permeability regions, severely reducing sweep efficiency. 3) Displacement efficiency responds non-monotonically to increasing pressure differential and displacing velocity, showing initial enhancement followed by reduction. Optimal parameters are: A. Pressure differential: 0.5-0.8 MPa; B. Displacing velocity: 0.3 mL/min. 4) Dominant controls on flood efficiency follow the hierarchy: Pressure differential > Displacing velocity > Permeability gradient. Development parameter optimization emerges as an effective strategy for enhancing waterflood performance.

*Corresponding Author

Email: liuzhonghua@cqust.edu.cn

1. Introduction

Low-permeability oil reservoirs represent a strategic development target for global hydrocarbon resource replacement, with reserves exhibiting consistent annual growth [1, 2]. However, fine pore-throat geometries and high flow resistance in these formations commonly yield elevated injection pressures, diminished single-well productivity, and inefficient water flood utilization during development [3-5]. Water flooding, while an economically viable enhanced recovery method for low-permeability reservoirs, remains constrained by complex geological and engineering factors [6]. Elucidating the dominant controlling factors and their mechanistic influence on water flood performance is imperative for optimizing development strategies and improving ultimate recovery [7-9].

Global research efforts have extensively investigated seepage mechanisms in low-permeability reservoirs, with increasing scholarly consensus validating the existence of threshold pressure gradients in such formations [10-12]. These gradients significantly constrain effective oil-phase flow through porous media and limit development strategy optimization, particularly given that oil-water biphasic flow exhibits substantially higher threshold pressures than single-phase flow [13-15]. Furthermore, permeability heterogeneity critically governs displacement efficiency [16]. Zhou Yingfang *et al*. [17-20]. established a multilayer commingled production model to derive the relationship between displacement efficiency and water cut across distinct reservoir strata Fig. (**1A**). This analysis demonstrates that: 1) Higher permeability strata exhibit accelerated waterflood front advancement; 2) Post-breakthrough displacement efficiency increases marginally; 3) Primary crude oil recovery occurs during high-water-cut stages >85%, with substantial efficiency gains emerging only after water cut surpasses 85%.

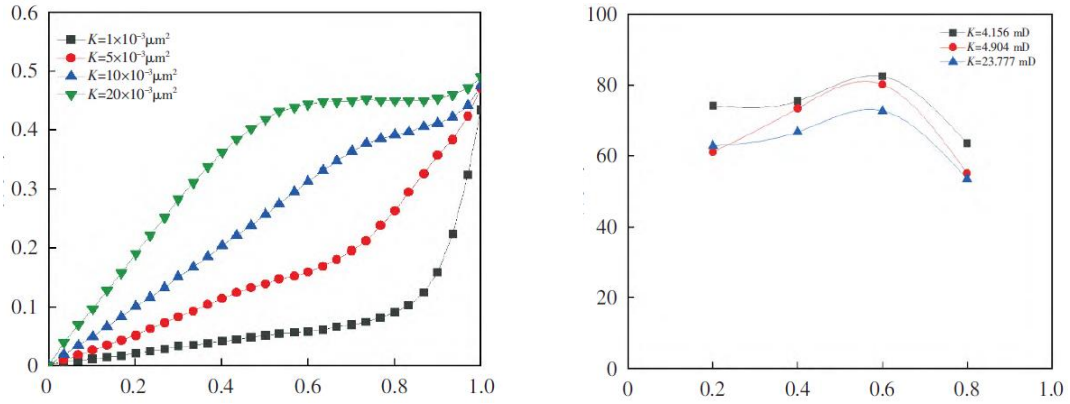

A. The impact of permeability

B. The impact of displacement speed

Figure 1: Investigation on the influencing factors of oil displacement efficiency in low-permeability reservoirs [20].

In response to characteristic challenges of low-permeability reservoirs, extensive theoretical and laboratory investigations have established an optimal displacement velocity range for waterflood operations in heterogeneous formations [21-23]. Analysis of the velocity-displacement efficiency relationship Fig. (**1B**) demonstrates reduced oil recovery when core displacement velocities deviate from the 0.6 mL/min optimum [17]. Constant-pressure displacement—a development approach distinct from constant-velocity methods—constitutes a principal waterflood technique for low-permeability reservoirs [24].

While laboratory studies remain limited, existing research indicates enhanced displacement efficiency with increasing injection pressure. Current understanding remains incomplete regarding dominant controls in low-permeability water flood development. The synergistic mechanisms governing sweep efficiency and displacement performance—particularly interactions between threshold pressure gradients, permeability heterogeneity, and displacement conditions pressure differential, velocity—require elucidation [24-29]. This study addresses these fundamental constraints through: 1) Laboratory determination of single-phase threshold pressure gradients; 2) Systematic analysis of permeability contrast, pressure differential, and displacement velocity impacts on water flood efficacy. Results clarify dominant controlling factors, providing a theoretical foundation and operational

parameter guidance for development design, thereby advancing efficient exploitation technologies for low-permeability reservoirs.

2. Experiment

2.1. Experimental Conditions and Design

1) Crude Oil: Target reservoir crude oil exhibiting a viscosity of 7.8 mPa·s under reservoir conditions 84°C.
2) Formation Water: Synthetic brine with mineralization of 8000 mg/L.
3) Core Preparation: Native core samples were processed as follows: End faces trimmed to precise cross-sectional geometry dimensions recorded using a core-facing machine(measure the length and diameter three times and take the average); Initial oven drying; Residual hydrocarbon extraction via high-temperature / high-pressure cleaning; Secondary drying; Permeability and porosity measurement by gas porosimetry gas permeability K and porosity Φ were determined using a CMS-300 porosimeter with a measurement uncertainty of < 0.5\% (Table **1**).
4) The experimental design is shown in Table **2**. To ensure statistical reliability, each parameter set was tested using representative core pairs or single cores based on the reservoir's permeability distribution.

Table 1: Experimental core data.

Core Number	Length, m	Diameter, cm	Permeability, mD	Porosity, %
1	0.046	2.48	1.750	15.88
2	0.049	2.48	1.639	17.80
3	0.048	2.49	26.935	15.08
4	0.044	2.49	13.384	16.92
5	0.049	2.51	0.410	11.20
6	0.049	2.50	0.124	7.50
7	0.050	2.49	73.116	20.44
8	0.049	2.50	17.377	14.51
9	0.048	2.51	27.187	18.18
10	0.046	2.52	5.236	14.44
11	0.049	2.48	33.147	16.81
12	0.043	2.50	24.792	18.87
13	0.049	2.48	22.543	15.73
14	0.048	2.51	10.567	12.89
15	0.033	2.49	3.873	15.32
16	0.050	2.51	5.049	16.36
17	0.032	2.49	2.124	13.76
18	0.047	2.52	0.023	11.41
19	0.049	2.51	0.014	5.56
20	0.049	2.52	0.078	11.57

Experimental parameters were designed as follows [30]: ① Permeability contrast (K_{max} / K_{min} = 1~5) based on target reservoir permeability distribution. ② Displacement velocities 0.01~1 mL/min derived from the target reservoir's injection rate of 0.3 mL/min, with five discrete sub-injection rates. ③ Pressure differentials established

by: a) Empirically determining threshold pressure gradients across permeability variants; b) Applying super-threshold pressure differentials at controlled increments.

Table 2: Research and design on the main control factors of water drive development efficiency.

	Main Control Influencing Factors		
	Permeability Ratio	**Displacing Velocity**	**Displacement Pressure Difference**
Experimental purpose	Study the influence of interlayer heterogeneity on oil displacement efficiency	Study on the Effect of Constant Speed Water Injection on Oil Displacement Efficiency	Study on the Effect of Constant Pressure Water Injection on Oil Displacement Efficiency
Experimental parameter design	1（1.750:1.639）	0.01mL/min	0.2MPa
	2（26.935:13.384）	0.1mL/min	0.3MPa
	3（0.410:0.124）	0.3mL/min	0.6MPa
	4（73.116:17.377）	0.6mL/min	0.8MPa
	5（27.187:5.236）	1mL/min	1.2MPa
Core number	1-10	16-20	11-15

2.2. Experimental Process and Steps

2.2.1. Experimental Equipment and Process

The main equipment for displacement experiment includes TC-100D constant speed and pressure pump, intermediate container, six way valve, core gripper, confining pressure pump, heating ring (Jiangsu Tuochuang Scientific Research Instrument Co., Ltd.), Pressure was monitored via high-precision sensors (Guangzhou Sennashi Instrument Co., Ltd.) with a range of 0–40MPa and a precision of ±0.05% Full Scale, etc. The process of parallel core displacement equipment is shown in Fig. (**2**) [31].

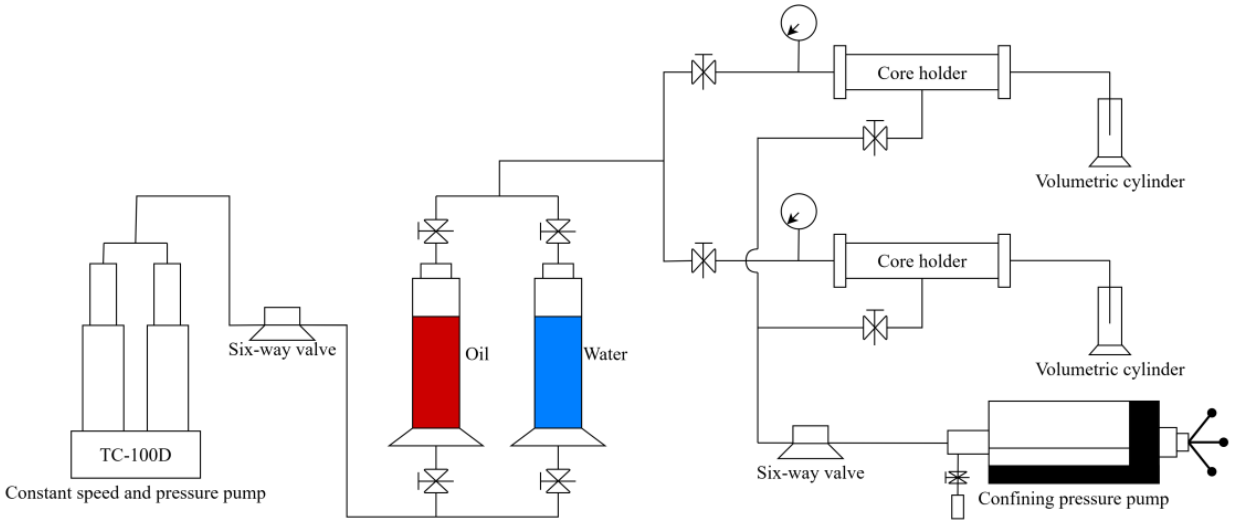

Figure 2: Flow chart of displacement equipment.

2.2.2. Test Steps for Starting Pressure Gradient of Low-permeability Core Oil Phase

The oil-phase threshold pressure gradient was determined as follows: ① Core saturation: Vacuum-saturate prepared cores with formation water; calculate porosity. ② Initial fluid displacement: mount core in holder under 3 MPa confining pressure. Displace formation water by crude oil injection at 0.1 mL/min until aqueous effluent ceases. Determine irreducible water saturation. ③ Aging: Thermally equilibrate at reservoir temperature for 24

hours. ④ Gradient measurement: Inject crude oil at 0.01 mL/min while continuously monitoring inlet (Pin) and outlet (Pout) pressures. The differential pressure ($\triangle P = P_{in} - P_{out}$) at initial hydrocarbon production defines the threshold pressure. The gradient is calculated as ΔP/L (L=core length) [32].

2.2.3. Experimental Steps for Water Flooding Oil

Water flood displacement experiments were conducted per the schematic in Fig. (**2**), utilizing parallel core holder configurations. Prepared cores Table **1** followed the experimental matrix in Table **2**. Cores previously tested for oil-phase threshold pressure Section 2.2.2 underwent additional 24-hour aging prior to use. Experiments proceeded as follows with real-time monitoring of displacement duration, injected/produced volumes, and pressure [33, 34].

1) Permeability Contrast Effect: Five core assemblies (permeability contrast K_{max} / K_{min} = 1–5) were waterflooded at 0.3 mL/min. Termination occurred at 90% aqueous phase fraction in effluent.
2) Velocity Effect: Cores were flooded at prescribed rates Table **2** under constant-rate mode. Termination criterion: 90% aqueous phase fraction.
3) Pressure Differential Effect: Target pressure differentials Table **2** were applied via constant-pressure injection. Termination at 90% aqueous phase fraction.

3. Result and Analysis

3.1. Starting Pressure Gradient of Single Oil Phase in Low-permeability Rock Core

The oil-phase threshold pressure gradient quantifies crude oil-rock interactions and defines the minimum energy threshold for flow initiation in porous media. Following the methodology in Section 2.2.2, threshold pressure gradients were determined across varying permeability conditions Fig. (**3**).

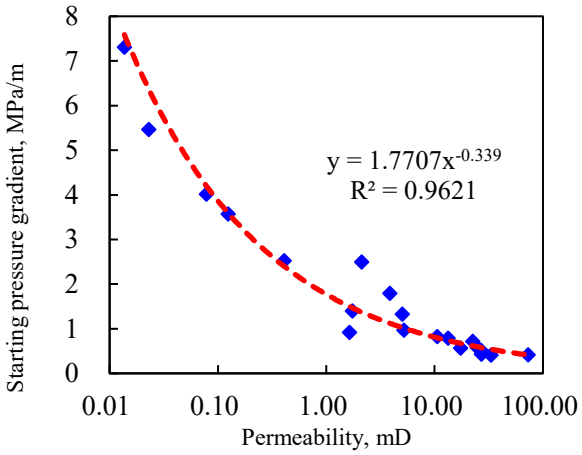

Figure 3: Starting pressure gradient at different permeabilities.

The oil-phase threshold pressure gradient data in Fig. (**3**) exhibit a power-law relationship with permeability, where the gradient increases inversely with decreasing permeability. For the target reservoir core permeability≈ 0.1mD, crude oil mobilization requires exceeding a threshold pressure gradient of 3.86 MPa/m. At 1 mD permeability, the required gradient is 1.77 MPa/m. For cores with average permeability 13 mD, Table **1**, a threshold gradient of 0.74 MPa/m must be exceeded to achieve crude oil mobilization.

These results demonstrate the inherent challenges in efficiently developing low-permeability reservoirs. Increased permeability contrast correlates with greater divergence in crude oil threshold pressure gradients, which subsequently amplifies variation in displacement efficiency. Systematic experimental investigation of permeability contrast effects and displacement methodologies is therefore critically warranted [35, 36].

3.2. The Impact of Permeability Gradient on the Effectiveness of Water Injection Development

Reservoir heterogeneity represents a key control on waterflood displacement efficiency. Fig. (**4A**) demonstrates waterflood performance across varying permeability contrasts in parallel cores, while Fig. (**4B**) illustrates corresponding displacement pressure differentials.

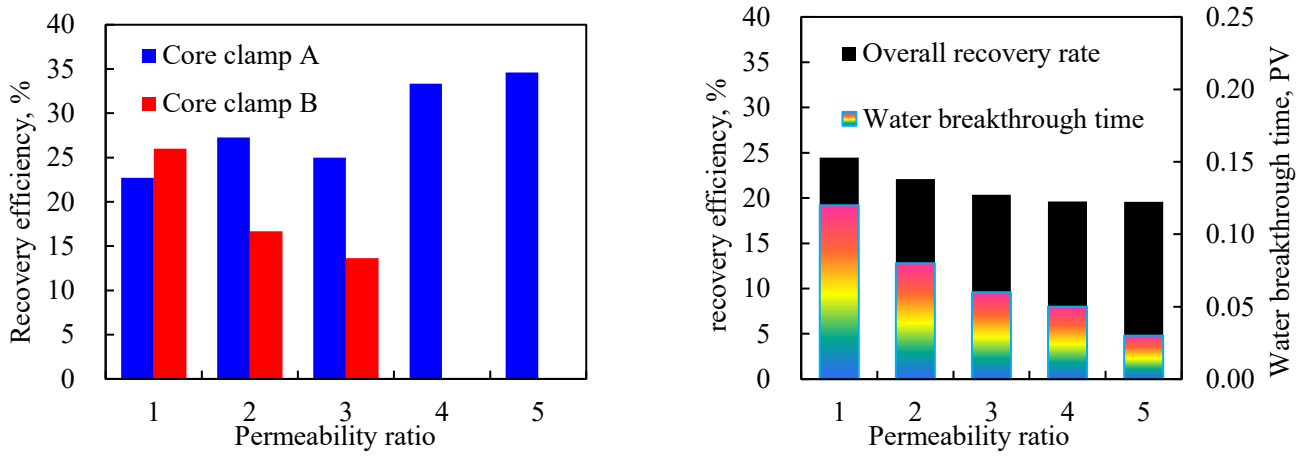

A. Single core water drive efficiency

B. Parallel core displacement efficiency and breakthrough time for water injection

Figure 4: The influence of permeability difference on oil displacement efficiency.

Fig. (**4**) demonstrates that increasing permeability contrast in parallel cores significantly diverges waterflood sweep efficiency. Table **2** further confirms that displacement efficiency remains comparable when permeabilities are similar. At a permeability contrast of 2, displacement efficiency differs by 10%. When contrast exceeds 3 (e.g., contrast = 4), negligible oil production occurs from low-permeability cores. Injected water preferentially flows through high-permeability cores, establishing preferential flow pathways. Consequently, production becomes dominated by high-permeability cores, accounting for >30% of total output.

Overall core recovery decreases progressively with increasing permeability contrast Fig. (**4B**), blackbars. Analysis of water breakthrough timing Fig. (**4B**), coloredbars indicates that uniform permeability enables coherent frontal advancement, with breakthrough occurring at approximately 0.12 PV. This demonstrates how low-permeability environments constrain waterflood efficiency and limit preferential flow pathways. Permeability contrast exacerbates injected water channeling, directing most flow into high-permeability layers and causing early breakthrough. At permeability contrast = 5, water breakthrough occurs after only 0.03 PV injection, establishing highly localized flow conduits in high-permeability layers. Notably, injection pressures remain moderate under these conditions. The pressure differentials in Fig. (**5**) arise not from heterogeneity but from the core's intrinsic low-permeability characteristics—specifically the threshold pressure gradient. Experimental data confirm that injection pressure increases inversely with target core permeability [37, 38].

3.3. The Impact of Water Injection Methods on Development Effectiveness

3.3.1. The Influence of Displacement Pressure Difference on Water Injection Development Effect

Conventional waterflood operations inject water at specified wellhead pressures to maintain constant displacement pressure differentials. Consequently, assessing the influence of displacement pressure differential on waterflood performance is essential. Fig. (**6**) presents experimental results for varying displacement pressure differentials.

Fig. (**6**) demonstrates that the target core exhibits early water breakthrough during waterflood development. Post-breakthrough water cut increases rapidly, displaying characteristic convex profile curvature. This behavior indicates inherent breakthrough susceptibility and low displacement efficiency. The recovery curve further reveals

that significant production occurs primarily during initial waterflood stages before 0.5 PV injection. Waterflood recovery follows an inverted-U trend relative to increasing displacement pressure differential Fig. (**7**). This pattern arises from three mechanisms: 1) At low pressure differentials, energy primarily overcomes the oil-phase threshold pressure gradient, limiting capillary force contributions; 2) Moderate pressure differentials enhance viscous forces during displacement, suppressing capillary effects and stabilizing flood fronts to improve sweep efficiency; 3) Excessive differentials exacerbate viscous fingering and crossflow, establishing preferential flow pathways that reduce volumetric sweep efficiency.

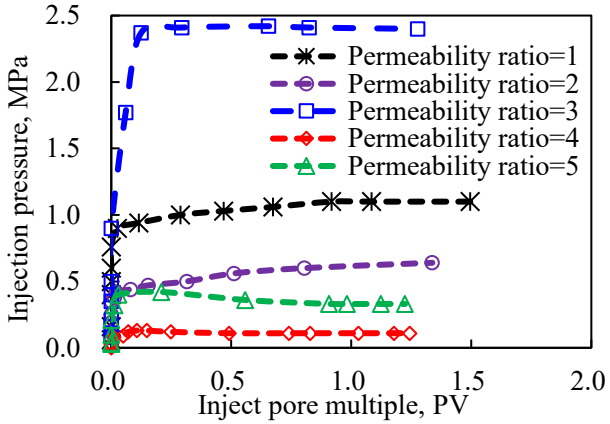

Figure 5: Displacement pressure at different permeability levels.

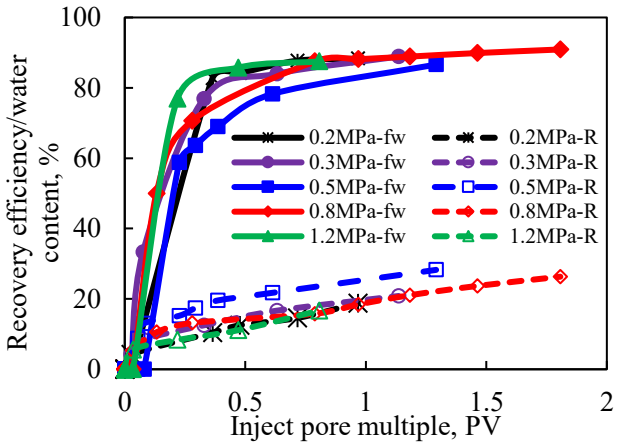

Figure 6: Oil displacement efficiency and water content variation curves under different pressure differentials.

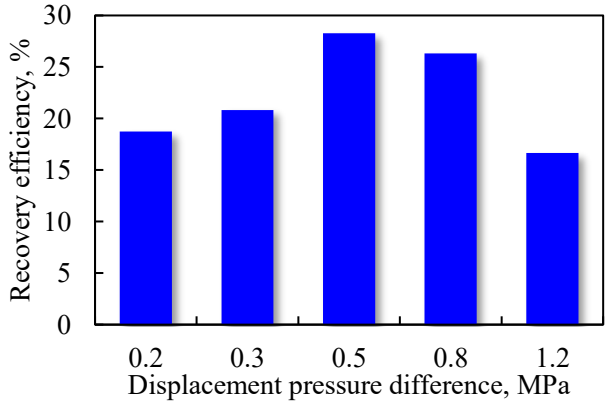

Figure 7: Oil displacement efficiency under different displacement pressure differentials.

There is an optimal displacement pressure difference range for water injection development in low-permeability reservoirs. The optimal displacement pressure difference obtained in this experiment is 0.5 MPa, which is roughly between 0.5 and 0.8 MPa.

Waterflood development in low-permeability reservoirs exhibits an optimal displacement pressure differential range. Experimentally, this optimum occurs at 0.5 MPa, with effective operation sustained between approximately 0.5 and 0.8 MPa.

3.3.2. The Influence of Displacement Speed on the Effectiveness of Water Injection Development

Varying injection pressures produce distinct displacement front velocities under reservoir conditions. Experimental measurements at these differential velocities quantify displacement efficiency, water cut, and pressure differential (Fig. **8**).

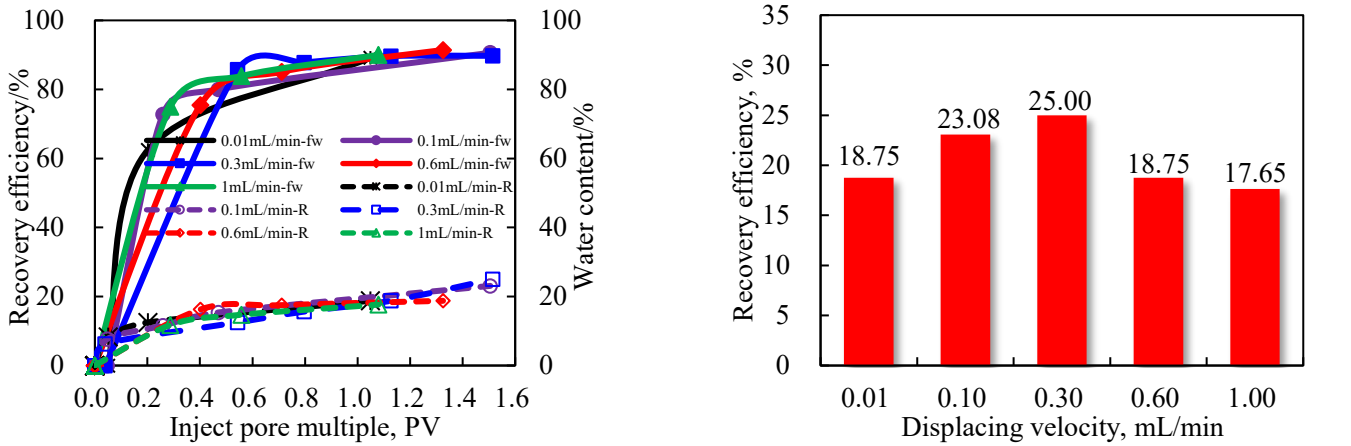

A. Oil displacement efficiency/water content curve

B. Oil displacement efficiency at different injection speeds

Figure 8: Oil displacement effect, water content, and displacement pressure at different displacement speeds.

Fig. (**8**) characterizes oil displacement behavior in low-permeability cores under varied injection rates. The water-cut profile Fig. (**8A**) indicates early breakthrough occurs after approximately 0.1 PV injection across all five core samples, followed by rapid water-cut escalation. Corresponding recovery curves demonstrate that primary oil production concentrates during initial waterflood stages, with incremental recovery declining sharply as water cut rises. Displacement efficiency exhibits a non-monotonic response to injection rates 0.01~1mL/min, showing an inverted-U trend with maximum recovery at 0.3 mL/min. This behavior reflects the dynamic equilibrium between viscous and capillary forces: 1) At low rates <0.3mL/min, capillary dominance restricts oil mobilization, reducing microscopic sweep efficiency; 2) Optimal rates 0.3mL/min enhance viscous forces to overcome capillary retention, improving displacement efficiency; 3) Excessive rates >0.3mL/min promote viscous fingering, establishing preferential flow pathways that bypass oil-saturated zones and reduce volumetric sweep.

The displacement pressure profile Fig. (**9**) demonstrates that effective pressure transmission in low-permeability cores requires first overcoming the threshold pressure gradient. The injection pressure curve exhibits a characteristic triphasic response: an initial rapid pressure increase, followed by rapid stabilization, and concluding with a gradual late-stage pressure rise. This sequence corresponds to: 1) Initial overcoming of the threshold pressure gradient; 2) Subsequent establishment of stable oil displacement; 3) Late-stage pressure elevation indicating effective waterflood performance.

3.4. Research on the Main Controlling Factors of Water Drive Efficiency in Low-permeability Reservoirs

The contributions of displacement pressure differential and front velocity to displacement efficiency exhibit non-monotonic behavior, characterized by initial enhancement followed by reduction. These contributions are quantified using the metric "displacement efficiency change rate per unit variable" $\Delta\eta/\Delta$variable, with comparative

results presented in Table **3**. The pressure differential demonstrates substantially greater influence on efficiency enhancement than front velocity.

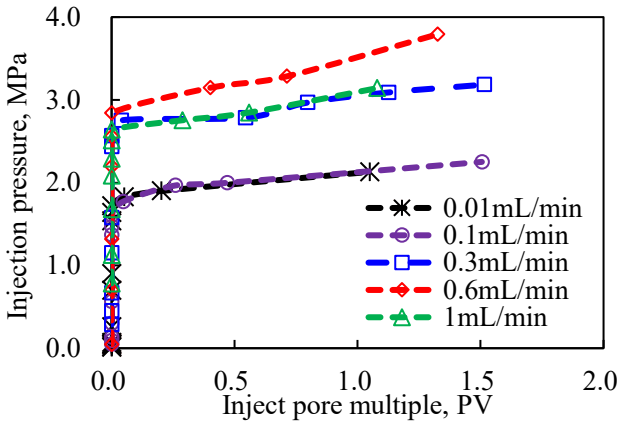

Figure 9: Injection pressure at different displacement speeds.

Table 3: Comparison of contribution of pressure difference and velocity to oil displacement efficiency.

	Calculation Content	Displacing Velocity, mL/min	Displacement Pressure Difference, MPa
Full range unit change rate	Total variation of independent variables	Δv=1.00−0.01=0.99	ΔP=1.2-0.2=1
	Maximum difference of dependent variable	ΔEv=25.00−17.65=7.35	$\Delta E_{\Delta P}$=28.26−16.67=11.59
	Efficiency changes of unit changes	ΔEv/Δv=7.35÷0.99≈7.42	$\Delta E_{\Delta P}/\Delta P$=11.59÷1=11.59
Unit change rate during the upward phase	Total variation of independent variables	Δv=0.3−0.01=0.29	ΔP=0.5-0.2=0.3
	Maximum difference of dependent variable	ΔEv=25.00−18.75=6.25	$\Delta E_{\Delta P}$=28.26−18.75=9.51
	Efficiency changes of unit changes	ΔEv/Δv=6.25÷0.29≈21.55	$\Delta E_{\Delta P}/\Delta P$=9.51÷0.3=131.7

Furthermore, comparative analysis of permeability gradient and displacement front velocity is conducted under controlled single-variable conditions. Parametric combinations with comparable independent variable ranges are selected for Grey Correlation Analysis to determine dominant controlling factors [39, 40]. Results are presented in Table **4**.

Table 4: Oil displacement efficiency under different factors.

ID	Permeability Ratio		Displacing Velocity	
	Experimental Parameters	Oil Displacement Efficiency, %	Experimental Parameters	Oil Displacement Efficiency, %
1	1.07	24.47	0.01mL/min	18.75
2	2.01	22.09	0.10mL/min	23.08
3	3.30	20.37	0.30mL/min	25.00
4	4.21	19.61	0.60mL/min	18.75
5	5.19	19.57	1.00mL/min	17.65
Contribution proportion	49.78%		50.22%	

Quantitative analysis reveals the permeability gradient contributes 49.78% to displacement efficiency, marginally lower than the 50.22% contribution from displacement front velocity. Comprehensive comparison

establishes the following hierarchy of controlling factors for flood efficiency in the target reservoir: Displacement pressure differential > Displacement front velocity > Permeability gradient. This indicates that while reservoir heterogeneity constrains flood efficiency, it constitutes a secondary controlling factor. Consequently, optimization of development parameters can substantially enhance reservoir flood efficiency. Specifically, selection of optimal displacement pressure differential enables maximized flood efficiency in the target reservoir.

4. Conclusion

1) The threshold pressure gradient G for single-phase oil flow in target reservoir cores exhibits a power-law relationship with permeability, indicating significant resistance to crude oil mobilization.
2) For permeability gradients $\geqslant$4, crude oil in low-permeability zones remains largely unswept. Water injection preferentially migrates through high-permeability regions, forming dominant channels that severely reduce sweep efficiency.
3) Displacement efficiency responds non-monotonically to increasing pressure differential and front velocity, exhibiting an initial enhancement followed by reduction. Optimal ranges are: A. Pressure differential: 0.5–0.8 MPa; B. Front velocity: 0.3 mL/min
4) Dominant controls on flood efficiency in low-permeability reservoirs follow the hierarchy: Pressure differential > Front velocity > Permeability gradient.

Conflicts of interest

The authors declare no conflict of interest.

Funding

Supported by China Postdoctoral Science Foundation (2023M744278) and Science and Technology Research Project of Chongqing Education Commission (KJQN202301518).

Data Availability and Materials

The data supporting the findings of this study are available from the corresponding author upon reasonable request.

Author Contributions

Shijie Zhu: Conceptualization, Writing—original draft, Funding acquisition;

Xijin Wang: Conceptualization;

Zhonghua Liu: Methodology, Resources, Writing—review and editing;

Heng Zhang: Formal analysis; Yuedi Wang: Data curation;

Yiqiang Pan: Writing—original draft;

Xiaoqing Wang: Writing—review and editing. All authors have read and approved the final manuscript.

References

[1] Zeng J, Huang H, Yuan S, Wu C. Low-porosity and low-permeability reservoirs characterization using low-frequency seismic attribute. Acta Geophys. 2020; 68(5): 1345-60. https://doi.org/10.1007/s11600-020-00474-5

[2] Ji B, Fang J. An overview of efficient development practices at low permeability sandstone reservoirs in China. Energy Geosci. 2023; 4: 100179. https://doi.org/10.1016/j.engeos.2023.100179

[3] Wang C, Sun Z, Sun Q, Zhang L, Zhang X. Comprehensive evaluation of waterflooding front in low - permeability reservoir. Energy Sci Eng. 2021; 9(9): 1394-1408. https://doi.org/10.1002/ese3.948

[4] Hassani K, Rostami B, Fathollahi A, Saeibehrouzi A. Soaking time effect on low salinity water injection in sandstone reservoirs: wettability, SEM, relative permeability, and waterflooding studies. Egypt J Pet. 2022; 31(2): 23-9. https://doi.org/10.1016/j.ejpe.2022.04.003

[5] Zhong X, Zhu Y, Jiao T, Qi Z, Luo J, Xie Y, *et al*. Microscopic pore throat structures and water flooding in heterogeneous low-permeability sandstone reservoirs: a case study of the Jurassic Yan'an Formation in the Huanjiang Area, Ordos Basin, Northern China. J Asian Earth Sci. 2021; 219: 104903. https://doi.org/10.1016/j.jseaes.2021.104903

[6] Wang X, Mao L, Kong X. Microscopic effects of long-term water injection on reservoir pore structure. Geoenergy Sci Eng. 2025; 253: 213952. https://doi.org/10.1016/j.geoen.2025.213952

[7] Zhang S. Research on the mechanism of decompression and augmented injection during waterflooding development in low permeability reservoirs. Open Pet Eng J. 2012; 5(1): 53-7. https://doi.org/10.2174/1874834101205010053

[8] Cui L. Research and application of potential tapping and efficiency enhancement technology in low permeability oilfield. 2021.

[9] Guo J, Wang H, Wang H. Investigating dynamic evolution of pore structures during long term water flooding via in-situ CT scanning: a case study of the Beibu-Gulf Basin in the South China Sea. Measurement. 2025; 118556. https://doi.org/10.1016/j.measurement.2025.118556

[10] Shi X, Wei J, Huang B, Zheng Q, Yi F, Yin Y, *et al*. A novel model for oil recovery estimate in heterogeneous low-permeability and tight reservoirs with pseudo threshold pressure gradient. Energy Rep. 2021; 7: 1416-23. https://doi.org/10.1016/j.egyr.2021.01.017

[11] Lei Q, Xiong W, Yuan J, Gao S, Wu YS. Behavior of flow through low-permeability reservoirs. In: SPE Europe/EAGE Annual Conference and Exhibition; 2008 Jun 9-12; Rome, Italy https://doi.org/10.2118/113144-MS

[12] Zeng B, Cheng L, Hao F. Experiment and mechanism analysis on threshold pressure gradient with different fluids. In: 34th Annual SPE International Conference and Exhibition; 2010 Jul 31-Aug 7; Tinaga - Calabar, Nigeria

[13] Zha W, Li D, Zeng Y, Lu D. Pressure transient behaviours of vertical wells in low permeability reservoirs with threshold pressure gradient. Int J Oil Gas Coal Technol. 2018; 18(3-4): 279-304. https://doi.org/10.1504/IJOGCT.2018.093131

[14] Jia J, Yu G, Li S, Peng R, Tang Y. Analysis of key controlling factors for water injection deficiency in low-permeability oil reservoirs: a case study of Chang-8 reservoir in Ordos Basin. Pet Reservoir Eval Dev. 2024; 14(6): 892-98.

[15] Dou H, Ma S, Zou C, Yao S. Threshold pressure gradient of fluid flow through multi-porous media in low and extra-low permeability reservoirs. Sci China Earth Sci. 2014; 57(11): 2808-18. https://doi.org/10.1007/s11430-014-4933-1

[16] Li M, Qu Z, Wang M, Wang R. The influence of micro-heterogeneity on water injection development in low-permeability sandstone oil reservoirs. Minerals. 2023; 13(12): 1533. https://doi.org/10.3390/min13121533

[17] Zhou Y, Fang Y, Wang X. A new method for calculating non-piston displacement efficiency in multilayered reservoir with waterflooding. Pet Geol Recovery Effic. 2009; 16(1): 86-89.

[18] Zhu W, Cao Z. Geological characteristics and waterflooding strategy for Yuanshi low permeability sandstone reservoir. Adv Mater Res. 2012; 594-597: 134-39. https://doi.org/10.4028/www.scientific.net/AMR.594-597.134

[19] Ma X, Bi Y, Jiang M, Li D, Gu X. Characteristics of water phase permeability variation in medium-low permeability oil reservoirs during high multiple waterflooding. Pet Reservoir Eval Dev. 2025; 15(1): 103-09.

[20] Zhao Y, Chen Z, Yang Y. Research progress on the law of waterflooding front migration in low-permeability tight reservoirs. Petrochem Ind Appl. 2024; 43(5): 1-8.

[21] Yan WH, Wang LM, Wang DZ, Shi XB. Optimization research on cyclic waterflooding in low permeability fractured reservoir. Adv Mater Res. 2012; 424-425: 220-22. https://doi.org/10.4028/www.scientific.net/AMR.424-425.220

[22] Wang D, Niu D, Li HA. Predicting waterflooding performance in low-permeability reservoirs with linear dynamical systems. SPE J. 2017; 22(5): 1596-1608. https://doi.org/10.2118/185960-PA

[23] Wang Z, Liu K, Zhang C, Yan H, Yu J, Yu B, *et al*. Integral effects of porosity, permeability, and wettability on oil-water displacement in low-permeability sandstone reservoirs—insights from X-ray CT-monitored core flooding experiments. Processes. 2023; 11(9): 2786. https://doi.org/10.3390/pr11092786

[24] Wang Z, Cao G, Bai Y. Development status and prospect of EOR technology in low-permeability reservoirs. Spec Oil Gas Reservoirs. 2023; 30(01): 1-13.

[25] Xu J, Jiang R. Non-Darcy flow numerical simulation for low-permeability reservoirs. In: 74th EAGE Conference and Exhibition incorporating EUROPEC 2012; 2012 Jun 4-7; Copenhagen, Denmark. SPE 154890. https://doi.org/10.2118/154890-MS

[26] Luo L, Cheng S. In-situ characterization of nonlinear flow behavior of fluid in ultra-low permeability oil reservoirs. J Pet Sci Eng. 2021; 203: 108573. https://doi.org/10.1016/j.petrol.2021.108573

[27] Civan F. Effective correlation of apparent gas permeability in tight porous media. Transp Porous Media. 2010; 82(2): 375-84. https://doi.org/10.1007/s11242-009-9432-z

[28] Deng J, Zhang R, Zhao X, Xu H, Ji P, Zhang Z, *et al*. Impact of permeability heterogeneity on methane hydrate production behavior during depressurization with controlled sand production. Energy Eng. 2025; 122(10): 4153-68. https://doi.org/10.32604/ee.2025.065906

[29] Zhang M, Li B, Zheng L, Xin Y, Xing W, Li Z. Experimental study on CO_2 flooding within a fractured low-permeability reservoir: impact of high injection rate. Fuel. 2025; 384: 134002. https://doi.org/10.1016/j.fuel.2024.134002

[30] Jia R. Experimental study on start-up pressure gradient of low permeability reservoirs in Fushan sag. Mud Logging Eng. 2018; 29(04): 20-23.

[31] Song L. Experimental study on water flooding in low-permeability reservoirs in XL block. Master's thesis. Heilongjiang: Northeast Petroleum University; 2021.

[32] Hu G, Hu S, Li Y, Liu Z. Effective displacement pressure of five-spot pattern by waterflood development in low permeability reservoir. Pet Reservoir Eval Dev. 2017; 7(03): 20-22.

[33] Al-Ibadi H, Stephen KD, Mackay EJ. Extended fractional-flow model of low-salinity waterflooding accounting for dispersion and effective salinity range. SPE J. 2019; 24(6): 874-888. https://doi.org/10.2118/191222-PA

[34] Zhao H, Xu L, Guo Z, Zhang Q, Liu W, Kang X. Flow-path tracking strategy in a data-driven interwell numerical simulation model for waterflooding history matching and performance prediction with infill wells. SPE J. 2020; 25(2): 1007-25. https://doi.org/10.2118/199361-PA

[35] Zha W, Li D, Zeng Y, Lu D. Pressure transient behaviours of vertical wells in low permeability reservoirs with threshold pressure gradient. Int J Oil Gas Coal Technol. 2018; 18: 279-304. https://doi.org/10.1504/IJOGCT.2018.093131

[36] Shi X, Wei J, Huang B, Zheng Q, Yi F, Yin Y, *et al*. A novel model for oil recovery estimate in heterogeneous low-permeability and tight reservoirs with pseudo threshold pressure gradient. Energy Rep. 2021; 7: 1416-23. https://doi.org/10.1016/j.egyr.2021.01.017

[37] Jiang Z, Ren H, Maimaitiming D, Wang Z, Dong H. Effects of water flooding speed on oil recovery efficiency and residual oil distribution in heterogeneous reservoirs. Pet Sci Technol. 2023; 41: 2362-75. https://doi.org/10.1080/10916466.2022.2108837

[38] Arab D, Kantzas A, Bryant SL. Water flooding of oil reservoirs: effect of oil viscosity and injection velocity on the interplay between capillary and viscous forces. J Pet Sci Eng. 2019; 182: 106691. https://doi.org/10.1016/j.petrol.2019.106691

[39] Zhu S, Shi L, Wang X, Liu C, Xue X, Ye Z. Investigation into mobility control mechanisms by polymer flooding in offshore high-permeable heavy oil reservoir. Energy Sources Part A. 2020; 46(1): 2024. https://doi.org/10.1080/15567036.2020.1797941

[40] Sun J, Liu D, Zhang L. Grey correlation analysis of the influencing factors on production decline in low permeability reservoirs. Spec Oil Gas Reservoirs. 2012; 19(02): 90-93.